



The diagnostic value of SPECT CZT quantitative myocardial blood flow in high-risk patients

Konstantin V. Zavadovsky, MD,^a Andrew V. Mochula, PhD,^a
Alina N. Maltseva, MD,^a Alla A. Boshchenko, MD,^a Andrew E. Baev, PhD,^a
Sergey L. Andreev, PhD,^a Evgeniy A. Nesterov, PhD,^b Riccardo Liga, MD,^c
and Alessia Gimelli, MD^d

^a Cardiology Research Institute, Tomsk National Research Medical Centre, Russian Academy of Sciences, Tomsk, Russia

^b National Research Tomsk Polytechnic University, Tomsk, Russia

^c Università di Pisa, Pisa, Italy

^d Fondazione Toscana, CNR Gabriele Monasterio, Pisa, Italy

Received May 25, 2020; accepted Sep 21, 2020

doi:10.1007/s12350-020-02395-8

Background. The objective of this study was to evaluate the accuracy of global MBF and MFR quantitation performed by myocardial perfusion scintigraphy (MPS) for the detection of multivessel coronary artery disease (CAD).

Methods. 52 CAD patients underwent CZT MPS, with the evaluation of MBF and MFR, followed by invasive coronary angiography (ICA). According to MPS and ICA results, all patients were divided into three groups: (1) non-obstructive CAD and normal MPS scan (control group) (n = 7), (2) one vessel disease (1VD) (n = 16), (3) multivessel disease (MVD) (n = 29).

Results. Global absolute MBF and MFR were significantly reduced in MVD patients as compared to those with 1VD [0.93 (IQR 0.76; 1.39) vs 1.94 (1.37; 2.21) mL·min⁻¹·g⁻¹, *P* = .00012] and [1.4 (IQR 1.02; 1.85) vs 2.3 (1.8; 2.67), *P* = .0004], respectively. The Syntax score correlated with global stress MBF ($\rho = -0.64$; *P* < .0001) and MFR ($\rho = -0.53$; *P* = .0003). ROC analysis showed higher sensitivity and specificity for stress MBF and MFR compared with semiquantitative MPS stress evaluation. Multivariate regression analysis showed that only stress MBF [OR (95% CI) 0.59 (0.42-0.82); *P* < .0003] was an independent predictor of MVD.

Conclusions. Quantitative myocardial blood flow values assessed with the use of CZT camera may identify high-risk patients, such as those with multivessel disease. (J Nucl Cardiol 2022;29:1051–63.)

Key Words: Multivessel disease • SPECT • CZT • CAD • myocardial ischemia • myocardial blood flow • myocardial flow reserve

Electronic supplementary material The online version of this article (<https://doi.org/10.1007/s12350-020-02395-8>) contains supplementary material, which is available to authorized users.

The authors of this article have provided a PowerPoint file, available for download at SpringerLink, which summarises the contents of the paper and is free for re-use at meetings and presentations. Search for the article DOI on SpringerLink.com.

The authors have also provided an audio summary of the article, which is available to download as ESM, or to listen to via the JNC/ASNC Podcast.

Funding Contribution of Evgeniy A. Nesterov was funded by Tomsk Polytechnic University Competitiveness Enhancement

Program Grant (VIU-Laboratory No. 31 YAR-221/2018, RFMEFI62019X0001).

Reprint requests: Konstantin V. Zavadovsky, MD, Cardiology Research Institute, Tomsk National Research Medical Centre, Russian Academy of Sciences, Kievskaya Str 111A, Tomsk 634012, Russia; konstav@gmail.com

1071-3581/\$34.00

Copyright © 2020 American Society of Nuclear Cardiology.

Abbreviations

AC	Attenuation correction
CAD	Coronary artery disease
CZT	Cadmium-zinc-telluride
FFR	Fractional flow reserve
ICA	Invasive coronary angiography
MBF	Myocardial blood flow
MFR	Myocardial flow reserve
MPS	Myocardial perfusion scintigraphy
MVD	Multivessel disease
NAC	Non-attenuation correction
PET	Positron emission tomography
SPECT	Single-photon emission computed tomography

INTRODUCTION

Myocardial perfusion scintigraphy (MPS) on single photon emission computed tomography (SPECT) remains one of the most robust approaches for the detection of coronary artery disease (CAD). However, in specific groups of patients the diagnostic accuracy of MPS is lower than expected. In particular, in patients with multivessel disease (MVD) the sensitivity of MPS with standard SPECT may be reduced because of the possible underestimation of CAD extent due to balanced ischemia. The new cadmium-zinc-telluride (CZT) cameras seem to increase the accuracy in detecting MVD, as already shown by an initial report.¹ Interestingly, the evaluation of absolute myocardial blood flow (MBF) with positron emission tomography (PET) has been demonstrated as the most robust technique for the detection of MVD,² but low availability and high cost of cardiac PET hinder the wide spread of this method.³

More recently, some published papers demonstrated the feasibility of MBF evaluation with the new CZT cameras. Due to their hardware and software features, these cameras can be used as PET, allowing to perform PET-like dynamic acquisition and then to quantitate MBF and myocardial flow reserve (MFR).⁴

While information about the correlation with invasive coronary angiography (ICA),⁵ fractional flow reserve (FFR)^{6,7} and PET MBF^{6,8} has been demonstrated in several papers, the clinical value of these analysis is not well established, particularly in high risk patients.⁹ Interestingly, there is a lack of data related to the diagnostic value of MBF and MFR derived by CZT gamma-camera in terms of MVD diagnosing. To this purpose, this study aimed at evaluating the added value of SPECT CZT derived MBF and MFR assessment for the detection of MVD.

METHODS**Study Design**

Between October 2017 and November 2018, a total of 56 consecutive patients with known or suspected CAD were referred by clinicians to MPS evaluation were enrolled in the study.

Patients were selected from those who were submitted to MPS scan accordingly to 2019 ESC Guidelines for Chronic Coronary Syndromes. In particular, from all patients that required an MPS scan, we selected all patients with high risk of CAD and we submitted these patients to CZT scan plus MBF evaluation. Further patients were referred to diagnostic ICA due to clinical reasons. Four patients showed completely normal MPS scan and refused to be submitted to coronary angiography, being excluded from the final analysis. Patients with non-obstructed CAD but abnormal MPI were not included in the study. Accordingly, 52 patients underwent both CZT MPS with MBF and MFR calculation and invasive coronary angiography. The interval between MPS and coronary angiography was less than 3 weeks.

Patients with acute coronary syndrome, hemodynamic instability, severely symptomatic heart failure, known myocardial disease, moderate-to-severe cardiac valvular disease, atrial fibrillation, prior revascularization by CABG, contraindication to adenosine or iodine administration were excluded from the enrollment.

The study was approved by the Local Ethical Committee and conformed to the Declaration of Helsinki on Human Research. Written informed consent was obtained from every patient after explanation of the protocol, its aims, and potential risks.

Patient Preparation

Patients were instructed to refrain from caffeine and methylxanthine-containing substances and to avoid nitrates, calcium channel blockers and beta-blockers for at least 24 hours before the scan. All scans were performed after an overnight fasting.

MPS Acquisition Protocol

All patients were imaged in the supine position with arms placed over their heads. Before the first dynamic acquisition, a low-dose CT scan (tube voltage 120 kV, tube current 20 mA, rotation time 0.8 seconds, helical pitch 0.969:1, slice thickness 5 mm, and interslice interval on 5 mm) was performed for heart positioning and for attenuation correction.

Each patient underwent stress-rest CZT (Discovery NM/CT 570c; GE Healthcare, Haifa, Israel) imaging according to a single-day protocol.

3 MBq·kg⁻¹ of ^{99m}Tc Sestamibi were injected at rest using a syringe pump intravenously as a 5 mL bolus (injection rate 1 mL·s⁻¹) followed by saline flush (20 mL with the rate 2 mL·s⁻¹, using an automatic injector Ulrich Missouri XD 2001 Ulrich GmbH & Co. KG, Ulm, Germany). List mode ECG-gated dynamic data acquisition started just prior to the radiopharmaceutical bolus injection and acquired for 610 seconds.

After 40 minutes from rest tracer injection, a 7 minute long standard ECG-gated (16 framed per cardiac cycle) rest acquisition was performed using a dedicated patient positioning tool in order to obtain the same coordinates of the heart as in the previous scan. The stress study was performed immediately after.

After 2 minutes of intravenous infusion of adenosine (140 mcg·kg⁻¹·min⁻¹), a second dose of ^{99m}Tc Sestamibi (9 MBq·kg⁻¹) was injected and list mode dynamic data acquisition of 610 s was started just prior to the radiotracer injection. The infusion of adenosine continued for additional 2 minutes.¹⁰ After that, as for rest scan, patients were removed from the gamma-camera and a stress standard ECG-gated scan was acquired after 45 minutes from the tracer injection.

The quality of the dynamic data including time-activity curves was good in all patients. The mean ^{99m}Tc-MIBI dose at rest was 258.9 ± 42.9 MBq (range 192–390 MBq); at stress 776.9 ± 128.7 (range 576–1,170 MBq). The low-dose CT scan dose was 0.27 mSv. The mean effective radiation dose was 8.46 ± 1.37 mSv (range 6.41–12.75 mSv) per patient.

Invasive coronary angiography

All patients underwent quantitative coronary arteriography on an Axiom Artis coronary angiography system (Siemens; Erlangen, Germany). All coronary artery stenoses were quantitatively assessed using dedicated software by an experienced reader (AEB). Coronary artery stenosis ≥ 70% in major epicardial coronary arteries and ≥ 50% in left main coronary artery were considered as significant. Finally, the Syntax score was calculated as a global measure of CAD extent and severity.¹¹ Multivessel disease patient were defined as having 2 or 3 vessel disease (> 70% stenosis); left main CAD (> 50% stenosis).

DATA ANALYSIS

Conventional CZT Data Reconstruction

Low dose CT scans were transferred to Xeleris workstation to obtain attenuation correction maps. The alignment of perfusion and CT data was done with a visual control. CZT images were reconstructed on the dedicated workstation (Xeleris 4.0; GE Healthcare, Haifa, Israel) using maximum-penalized-likelihood iterative reconstruction (60 iterations; Green OSL α 0.7; Green OSL β 0.3) to acquire perfusion images in standard cardiac axes (short axis, vertical long axis, and horizontal long axis). The software Myovation for Alcyone (GE Healthcare, Haifa, Israel) was used for image reconstruction, and Butterworth post-processing filter (frequency 0.37; order 7) was applied to the reconstructed slices. The reconstruction was performed in 70 × 70 pixels matrix with 50 slices.

Raw MPS-CZT data at stress and at rest were visually analyzed for motion and attenuation artefacts. Stress/rest images were analyzed with a commercially available software package Corridor 4DM (University of Michigan, Ann Arbor, MI, USA). The calculation of MPS parameters was performed on both attenuation corrected (AC) and non-attenuation corrected (NAC) images.

Each of 17 segments was scored based on semiquantitative 5-point scoring system (from 0 = normal uptake to 4 = absent radiotracer distribution).¹² Accordingly, the sum of the stress scores of all segments (SSS) and the sum of the rest scores of all segments (SRS) were quantified. A summed difference score (SDS) was calculated as the difference between SSS and SRS. Moreover, a per-vessel analysis was also performed with estimation of regional scores (SS, SR and SD) for each coronary artery territory. The values of transient ischemic dilation (TID) ratio were estimated.

Analysis of Gated Images

LV functional analysis was performed from 16-frames reformatted images using commercially available software (Corridor4DM, Invia, Ann Arbor, MI). The LVEF as well as EDV and ESV during stress rest and were determined.

Dynamic CZT Data Analysis

Dynamic CZT imaging was processed as previously published⁷ with changes in framing and Renkin-Crone equation parameters. In brief, the acquired data were initially reconstructed (in 70 × 70 pixels matrix; 50 slices) and rebinned into 21 frames: 18 frames of 10 seconds each and 3 frames of 120 seconds each. The reframed and corrected (for stress dataset) dynamic images were reconstructed using penalized maximum likelihood expectation maximization iterative algorithm. Finally, the reconstructed dynamic images as well as CT attenuation correction maps were processed by 4DM Reserve (2015 version) application. The time-activity curves for the input function and whole left ventricular myocardium as well as for the left anterior descending

coronary artery (LAD), left circumflex coronary artery (LCX) and right coronary artery (RCA) vessel territories were generated semiautomatically. The region of interest (ROI) for input function was located on the valve plane and including parts of LV cavity and left atrium. Manual motion correction of dynamic dataset was performed in accordance with manufacturer's recommendation.¹³ The myocardial retention rate was estimated using generalized net retention model.^{14,15}

To convert the tracer retention rate to MBF values the Renkin-Crone flow model was used using parameters $\alpha = 0.880$, $\beta = 0.208$.¹⁴ The value of MFR was calculated as MBF ratio (MBF stress/MBF rest). Additionally, the absolute difference between stress MBF and rest MBF as flow difference (FD) was calculated.^{16,17} Rest and stress quantitative indexes were calculated with and without AC.

Determination of Intraobserver and Interobserver Reproducibility of the Quantitative Indexes

For intraobserver reproducibility 25 randomly selected patients with at least a 1-month interval between measurements were analyzed by an experienced nuclear radiologist (AM). To test interobserver reproducibility these patients were analyzed by two readers (KZ and AM).

Statistical Analysis

The distribution of continuous variables was checked by using the Shapiro-Wilk W-test. Continuous variables were expressed as mean \pm standard deviation and as median with quartiles (Q₂₅-Q₇₅). Kruskal-Wallis test was used to test differential distribution of data in three groups. The level of significance was adjusted for multiple testing using Bonferroni error correction. Spearman test was used to estimate the correlation coefficient between quantitative variables. To evaluate the independent predictors of MVD, forward-stepwise logistic regression analysis was used with an entry criterion of $P < .05$ and a removal criterion of $P > .1$. Accuracy of MVD detection was assessed by receiver operator characteristic (ROC) analysis, reporting areas under the curve (AUC) and their associated 95% confidence intervals (CIs). The best values in the prediction of MVD were defined as the cut-off point having the highest Youden Index. The values of areas under curve were compared by the DeLong method. Intra- and interobserver reproducibility was assessed with intraclass correlation coefficients (ICC). Values were considered statistically significant when P was $< .05$. Statistical analyses were performed using SPSS statistical software 19.0 (SPSS, Inc., Chicago, IL, USA) and MedCalc version 17.4 (MedCalc Software, Mariakerke, Belgium).

RESULTS

Study Population

The clinical characteristics of patients are presented in the Table 1. Based on invasive coronary angiography and MPS data all patients were divided into three groups: (1) patients without obstructive CAD and SSS < 4 (control group); (2) patients with significant CAD (stenosis $\geq 70\%$) in one major epicardial coronary artery (one vessel CAD group, 1VD); (3) patients with at least one $\geq 70\%$ stenosis in two or more major epicardial coronary artery as well as patients with $\geq 50\%$ LMA stenosis were included in the multivessel disease (MVD) group.

ICA Results

According to per-patient analysis 6 (11%) patients had $\geq 50\%$ stenosis in the LMA; 35 patients showed significant lesions in the LAD, 26 patients in the LCX and 23 patients in the RCA. The value of Syntax score was 15.0 (IQR 8.0; 22.0). At per-vessel analysis, in 1VD patients a significant coronary stenosis was found in 13 LAD vessels, 3 LCX vessels and 0 RCA vessel; while in the MVD group 6, 24, 24 and 23 obstructive lesions were detected in LMA, LAD, LCX and RCA vessels, respectively.

MPS Analysis

The results of conventional and quantitative MPS parameters are presented in Table 2.

Attenuation corrected SSS and SDS did not differ significantly between 1VD and MVD groups whereas SRS and TID ratio were comparable between all three groups. On the contrary, NAC SSS was significantly higher in MVD group compared to 1VD one ($P = .02$). At quantitative analysis, both AC and NAC stress MBF and MFR were significantly lower in patients with MVD than in control group or 1VD. Among functional indexes, only stress ESV and EF were significantly lower in MVD when compared to 1VD. An example of a patient with MVD is presented in Figure 1.

A significant correlation between MPS results (with AC) and Syntax score was found. In particular, the Syntax score correlated with stress MBF ($\rho = -0.64$; $P = .000001$), MFR ($\rho = -0.53$; $P = .0003$), FD ($\rho = -0.54$; $P = .0002$), SSS ($\rho = 0.48$; $P = .0002$), SDS ($\rho = 0.44$; $P = .001$), and stress EF ($\rho = -0.41$; $P = .01$). The Syntax score showed lower correlations with NAC quantitative MPS parameters as compared to those with AC. No statistically significant correlation between

Table 1. Patient characteristics

Demographics and clinical characteristics	All patients	Control group	1VD	MVD	P (control group vs 1VD)	P (1VD vs MVD)
Number of patients	52	7	16	29		
Age (years)	60.6 ± 7.5	60.2 ± 4.9	59.1 ± 7.44	61.3 ± 8.5	NS	NS
Male gender, n (%)	39 (75)	6 (86)	11 (69)	22 (76)	NS	NS
Known CAD, n (%)	30 (58)	0 (0)	10 (62)	20 (69)	.007	NS
Previous MI, n (%)	35 (67)	0 (0)	10 (63)	25 (86)	.007	NS
Cardiovascular symptoms						
Typical angina, n (%)	20 (38)	0 (5)	5 (31)	15 (52)	NS	NS
Atypical angina, n (%)	23 (44)	6 (86)	7 (44)	10 (34)	NS	NS
Non-anginal chest pain, n (%)	9 (17)	1 (14)	4 (25)	4 (14)	NS	NS
NYHA class						
0, n (%)	11 (21)	7 (100)	2 (12.5)	2 (7)		
I, n (%)	6 (11)		2 (12.5)	4 (14)		
II, n (%)	30 (58)		11 (69)	19 (65)		
III, n (%)	5 (10)		1 (6)	4 (14)		
Cardiovascular risk factors						
Family history of CAD, n (%)	13 (25)	1 (14)	4 (25)	8 (27)	NS	NS
Diabetes, n (%)	15 (29)	2 (29)	4 (24)	9 (31)	NS	NS
Hypercholesterolemia, n (%)	20 (38)	3 (43)	9 (56)	13 (45)	NS	NS
Hypertension, n (%)	46 (88)	5 (71)	12 (75)	29 (100)	NS	.01
Smoking, n (%)	31 (60)	1 (14)	11 (68)	19 (66)	.02	NS
Body mass index (m ²) (IQR)	28.7 (26.1; 32.7)	26.3 (23.8; 30.35)	29.7 (25.9; 31.7)	28.4 (26.8; 33.6)	NS	NS
Coronary data						
Syntax score (IQR)	14.5 (7.5; 22.5)	5 (5.0; 6.5)	9.0 (7.0; 12.0)	21.5 (17.7; 27.1)	.004	.0002

All data are presented as mean ± SD, median and interquartile range (IQR) and n (%)
1VD, one vessel disease; CAD, coronary artery disease; MI, myocardial infarction; MVD, multivessel disease; NYHA, New York Heart Association

the Syntax score and visual NAC MPS indexes were found (Supplementary Material).

Predictors of MVD

History of previous myocardial infarction, AC SSS, SRS, stress MBF, MFR, FD, stress EF resulted the only variables predicting MVD (Table 3). However, multivariate logistic regression analysis showed that only AC stress MBF [OR (95% CI) 0.59 (0.42-0.82); *P* < .0003] was an independent predictor of MVD. According to univariate regression analysis NAC SSS, SDS stress MBF, MFR, FD allowed to predict MVD even if the

statistical power of the same parameter evaluated with AC (except SDS) is higher, as indicated with the odds ratios (Supplemental Table 1). In accordance to AC data analysis, multivariate logistic regression demonstrated that only NAC stress MBF was an independent predictor of MVD, however the prognostic significance was lower compared to AC stress MBF [OR (95% CI) 0.87 (0.77-0.97); *P* = .01].

Representative ROC curves for the evaluation of the accuracy of the most important scintigraphic predictors of MVD are shown in Figure 2. The AC stress MBF ROC curve showed the higher accuracy (*P* = .03) when compared to the AC SSS ROC curve,

Table 2. Myocardial perfusion scintigraphy results

MPI and blood flow parameters	All patients	Control group (n=7)	1VD (n = 19)	MVD (n = 27)	P value Kruskal-Wallis test	P, multiple comparison mean test		
						Control group-1VD	Control group-MVD	1VD-MVD
MPS parameters								
AC SSS	8 (4; 10)	1 (0; 2)	7 (5; 9.5)	8 (7; 12)	.0001	.0003	.00009	NS
AC SRS	2.0 (0; 3.5)	1.0 (0.0; 2)	2.0 (0; 3)	2.0 (0; 6)	NS	NS	NS	NS
AC SDS	4 (2; 8)	0 (0; 2)	4 (4; 8)	6 (4; 9)	.001	.0002	.0012	NS
NAC SSS	8.00 (5.0; 12.0)	3.0 (2.0; 4.0)	7.00 (5.0; 10.0)	10.5 (7.00; 15.00)	.0007	.01	.00016	.02
NAC SRS	4.0 (2.0; 8.0)	2.0 (2.0; 2.0)	4.0 (1.5; 8.5)	5.0 (3.0; 8.0)	NS	NS	.01	NS
NAC SDS	5.0 (2.0; 6.0)	1.0 (1.0; 3.0)	4.5 (2.0; 5.5)	5.0 (4.0; 7.0)	.0108	.03	.0027	NS
TID ratio	1.07 (0.94; 1.18)	1.07 (0.84; 1.11)	1.07 (0.96; 1.20)	1.12 (0.96; 1.23)	NS	NS	NS	NS
MPS functional								
Stress EDV (mL)	114 (89; 145)	106 (101; 128)	98 (83;131)	130 (89; 164)	NS	NS	NS	NS
Stress ESV (mL)	40 (27; 54)	40.0 (22; 41)	30.05 (22; 43)	50 (36; 65)	.04	NS	NS	.033
Stress EF (%)	65 (61; 73)	68.0 (62; 78)	70 (63; 73)	62 (55; 67)	.04	NS	NS	.023
Rest EDV (mL)	106 (83; 128)	122 (92; 129)	99 (73; 124)	111 (85; 140)	NS	NS	NS	NS
Rest ESV (mL)	32 (22; 47)	37 (22; 47)	28 (17; 38)	35 (26; 47)	NS	NS	NS	NS
Rest EF (mL)	70 (63; 73)	70 (61; 72)	72 (62; 75)	67 (63; 75)	NS	NS	NS	NS
Absolute parameters with AC								
Stress MBF (mL·min ⁻¹ ·g ⁻¹)	1.38 (0.9; 2.03)	2.2 (2.13; 2.3)	1.94 (1.37;2.21)	0.93 (0.76;1.39)	< .0001	.01	.00011	.00012
Rest MBF (mL·min ⁻¹ ·g ⁻¹)	0.81 (0.61; 0.95)	0.82 (0.78; 0.92)	0.89 (0.65; 0.96)	0.71 (0.53; 0.84)	NS	NS	NS	NS
MFR	1.85 (1.23; 2.43)	2.64 (2.5; 2.82)	2.3 (1.8; 2.67)	1.4 (1.02; 1.85)	< .0001	.03	.00022	.0004
FD (mL·min ⁻¹ ·g ⁻¹)	0.73 (0.15; 1.18)	1.38 (1.34; 1.5)	1.06 (0.85; 1.39)	0.23 (0.07; 0.69)	< .0001	.02	.00029	.0003
Absolute parameters with NAC								
Stress MBF (mL·min ⁻¹ ·g ⁻¹)	1.94 (1.41; 2.72)	2.78 (2.50; 3.03)	2.60 (1.68; 3.09)	1.50 (1.23; 2.13)	.0052	NS	.014	.0067

Table 2. continued

MPI and blood flow parameters	All patients	Control group (n=7)	1VD (n = 19)	MVD (n = 27)	P value Kruskal-Wallis test	P, multiple comparison mean test		
						Control group-1VD	Control group-MVD	1VD-MVD
Rest MBF (mL·min ⁻¹ ·g ⁻¹)	0.97 (0.58; 1.21)	0.97 (0.93; 1.12)	0.98 (0.51; 1.23)	0.92 (0.55; 1.25)	NS	NS	NS	NS
MFR	2.13 (1.56; 2.82)	2.71 (2.64; 2.87)	2.59 (2.17; 3.02)	1.87 (1.23; 2.25)	.018	NS	.04	.017
FD (mL·min ⁻¹ ·g ⁻¹)	0.97 (0.39; 1.61)	1.81 (1.69; 1.91)	1.28 (1.00; 1.81)	0.55 (0.29; 1.16)	.001	NS	.002	.004

All data are presented as median and interquartile range (IQR). 1VD, one vessel disease; MVD, multivessel disease; AC, attenuation correction; NAC, non-attenuation correction; MPS, myocardial perfusion scintigraphy; SSS, summed stress score; SRS, summed rest score; SDS, summed difference score; T1D, transient ischemic dilation ratio; FD, flow difference; EDV, end diastolic volume; EF, ejection fraction; MBF, myocardial blood flow; mL·min⁻¹·g⁻¹, milliliters per minute per gram; MFR, myocardial flow reserve

indicating the added value of quantification of absolute MBF versus the semiquantitative MPS analysis. ROC curves for NAC SSS, stress MBF, MFR and FD are presented on Figure 1 in Supplementary Material. In line with AC data, NAC stress MBF allowed identifying MVD better than NAC SSS, with slightly greater sensitivity and lower specificity (Supplemental Figure 1).

Finally, per-vessel analysis confirmed the role of absolute MBF in detecting MVD (Figure 3), showing that regional AC stress MBF value correlated better than semiquantitative variables with severity of coronary stenosis.

Reproducibility Test Results

ICC values showed good inter-operator reproducibility for global rest MBF (ICC 0.86, 95% CI 0.77-0.91), global stress MBF (ICC 0.82, 95% CI 0.74-0.88), and global MFR (ICC 0.89, 95% CI 0.82-0.93). Intraobserver reproducibility also showed good ICC results for global rest MBF (ICC 0.84, 95% CI 0.76-0.89), global stress MBF (ICC 0.79, 95% CI 0.67-0.88), and global MFR (ICC 0.81, 95% CI 0.73-0.88)

DISCUSSION

The main finding of this study is the additional diagnostic value of absolute stress MBF derived by CZT camera in the evaluation of obstructive lesion burden. In particular, the use of stress MBF can be of help in the detection of patients with multivessel disease. A correlation between stress MBF with the Syntax score has been also revealed. To our knowledge, this is the first report where stress MBF obtained by CZT SPECT was an independent predictor of high-risk patients. Furthermore, the direct comparison between semiquantitative MPS indexes such as SSS and SDS and quantitative CZT SPECT derived indexes was performed in patients with one- and multivessel disease.

In line with earlier works^{5,18} better diagnostic accuracy of quantitative dynamic SPECT indexes such as MBF and MFR versus visual parameters was revealed. Corresponding with previous studies we demonstrated the feasibility of CZT SPECT in assessment of stress MBF and MFR in CAD patients and decreased values of global stress MBF in multivessel disease.^{5,6,9} Moreover, previous studies enrolled small number of high-risk patients and showed mainly the diagnostic value of MFR. In this study, higher accuracy of stress MBF to detect high-risk patients compared to low risk patients has been shown.

In our study the correlation of stenosis severity versus regional stress MBF was higher by using AC

Global Results

A

Region	Mean		Flow (ml/min/g)		Reserve
	MC Str	MC Rst	MC Str	MC Rst	
LAD	71 %	75 %	1.39	1.35	1.02
LCX	69 %	62 %	1.24	0.93	1.33
RCA	82 %	91 %	1.59	1.40	1.14
TOT	74 %	76 %	1.41	1.25	1.12

Algorithm (MC Str): GE 530c Tc-99m NetRet Leppo AC
Algorithm (MC Rst): GE 530c Tc-99m NetRet Leppo AC

B

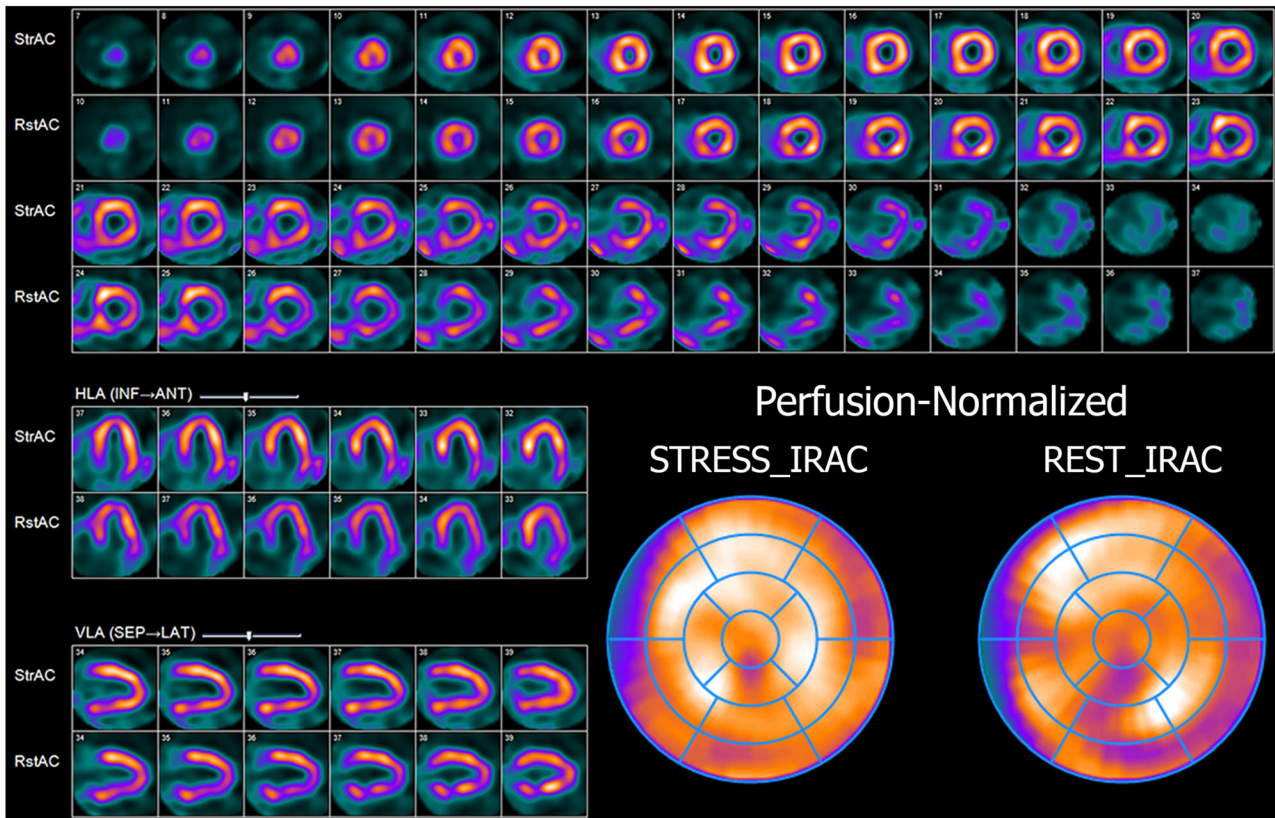


Figure 1. Example of MPS results in patient with multivessel coronary artery disease. A 69 years old male with multivessel disease (LAD 95%, LCX 90% and RCA 95%). (A) Result of quantitative dynamic SPECT. The obtained results indicate a normal pattern of the rest AC values of MBF, with a minimum increase of the same values after stress, with a reduction in the MFR. (B) The qualitative evaluation shows perfusion abnormalities in the postero-lateral wall, with an underestimation of the ischemic burden. AC, attenuation correction; LAD, left anterior descending artery; LCX, left circumflex artery; MC, motion correction; $mL \cdot min^{-1} \cdot g^{-1}$, milliliters per minute per gram; RCA, right coronary artery; Reserve, coronary flow reserve; Rst, rest; Str, stress; TOT, total value.

images compared to NAC. Moreover, the accuracy of AC data in identifying MVD was higher rather than the use of NAC data. These results confirm the previously published data regarding more accurate MBF and MFR

estimation by using SPECT CZT with attenuation correction.^{19,20} Our results suggest that the use of AC could be of help when CZT SPECT is used for MVD identification.

Table 3. Univariate predictors of multivessel disease

Characteristic	OR (95% CI)	P value
Age (years)	1.05 (0.99-1.12)	.07
Male gender	1.10 (0.3-3.91)	.87
Previous MI	8.1 (2.12-31.0)	.03
Smoking, current and former	2.03 (0.65-6.33)	.2
Diabetes mellitus	1.27 (0.37-4.31)	.69
Hypercholesterolemia	0.74 (0.21-2.23)	.59
Family history of CAD	1.37 (0.38-4.94)	.62
AC SSS	1.28 (1.08-1.52)	.004
AC SRS	1.29 (1.00-1.65)	.04
AC SDS	1.17 (0.98-1.40)	.06
AC stress MBF (per each 0.1 mL·min ⁻¹ ·g ⁻¹)	0.70 (0.59-0.84)	.0001
AC MFR (per each 0.1)	0.74 (0.63-0.87)	.0005
AC FD (per each 0.1 mL·min ⁻¹ ·g ⁻¹)	0.7 (0.58-0.84)	.0002
Stress EF (%)	0.9 (0.83-0.99)	.03
EDV (mL)	1.0 (0.99-1.03)	.08
ESV (ml)	1.04 (0.99-1.08)	.06

The dependent variable was the presence of multivessel disease

MFR, myocardial flow reserve; CI, confidence interval; EDV, end diastolic volume; EF, ejection fraction; ESV, end systolic volume; FD, flow difference; MBF, myocardial blood flow; MI, myocardial infarction; mL·min⁻¹·g⁻¹, milliliters per minute per gram; OR, odds ratio; SDS, summed difference score; SRS, summed rest score; SSS, summed stress score

The Clinical Value of Absolute MBF Assessment

Currently, PET imaging is the most established and clinical proofed approach to assess MBF and MFR.^{21,22} It is also known that stress MBF is a diagnostic and prognostic factor in patients with microvascular dysfunction.²³ According to recent data,^{24–26} stress MBF has also prognostic significance in terms of cardiac death and MI.

Interestingly, absolute MBF has been demonstrated of having a better accuracy in the evaluation of patients with stable angina and intermediate risk of CAD as compared not only to semiquantitative analysis but also to MFR.^{27,28} Moreover, stress MBF was an independent predictor of the left ventricular function impairment both in patients with and without previous MI.²⁹

The quantification of MBF is relevant in patients with multiple coronary artery lesion or microvascular dysfunction, because of the relatively high prevalence of false negative results at semiquantitative analysis (i.e. balanced ischemia) with standard SPECT. To this aim, several PET studies demonstrated that quantitative assessment of perfusion imaging is superior in comparison to qualitative analysis in terms of diagnostic accuracy.^{30,31} On the contrary, myocardial perfusion evaluation by SPECT remains one of the most used

technique due to its availability and the lower costs. Nevertheless, standard SPECT does not allow to quantify absolute MBF and, as previously published, may underestimate the severity of CAD, particularly in patients with extensive CAD.³²

The new CZT cameras dedicated to MPS allow to acquire dynamic images⁴ and thus to quantify MBF.^{20,33,34}

Accordingly, the use of this camera could overcome the limits of PET availability and cost for the evaluation of absolute MBF and MFR, making possible to quantify these values for clinical purpose.

CZT Quantification of MBF for the Evaluation of MVD

The results of our study indicate that the evaluation of CZT regional and global MBF added a significant value in the risk stratification of the different groups of patients. This result is of relevance in terms of clinical decision making, because it allows to detect patients with MVD during a functional test and thus to evaluate the risk of each patient.

Previous study indicated that there was a correlation between absolute and normalized MBF as well as MFR with ICA data,⁵ and the authors underlined the value of

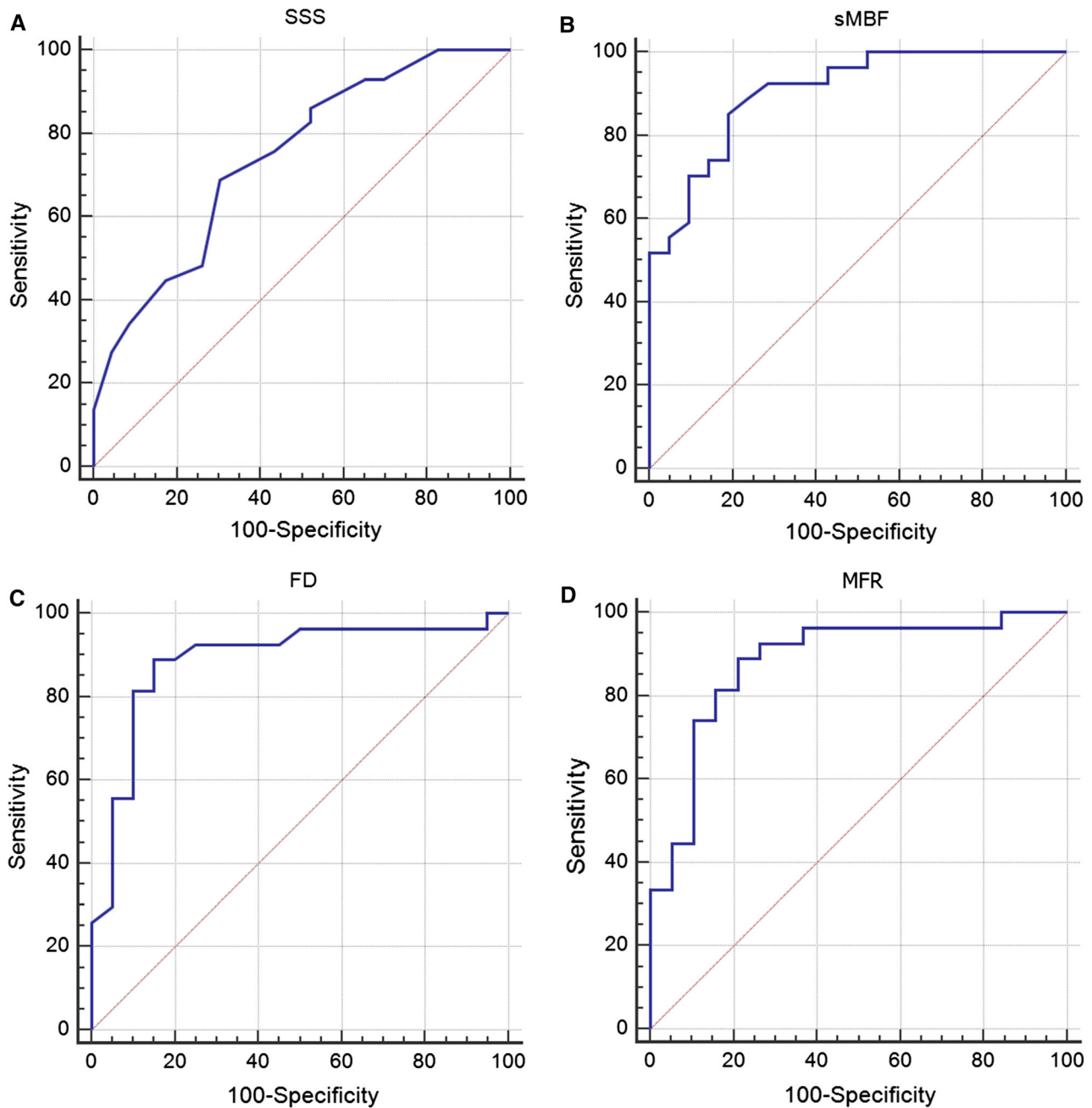


Figure 2. ROC curves for AC SPECT parameters comparing global left ventricular perfusion and flow parameters for MVD identification. (A) The ROC curve for the SSS values indicates a cut off of > 7 as the best predictor for the identification of MVD (AUC = 0.74; 95% CI 0.6-0.85; $P = .0004$; sensitivity 69%; specificity 69%); (B) the ROC curve for stress MBF demonstrates that the cut-off of ≤ 1.57 is the best predictor of MVD (AUC = 0.9; 95% CI 0.78-0.97; $P < .0001$; sensitivity 85.2%; specificity 81.0%); on the bottom (C) and (D) indicate the best cut-off value for FD (AUC = 0.88; 95% CI 0.76-0.96; $P < .0001$; cut-off value ≤ 0.83 ; sensitivity 88.9%; specificity 85.0%) and MFR (AUC = 0.88; 95% CI 0.78-0.96; $P < .0001$; cut-off value ≤ 1.91 ; sensitivity 88.9%; specificity 80.0%), respectively.

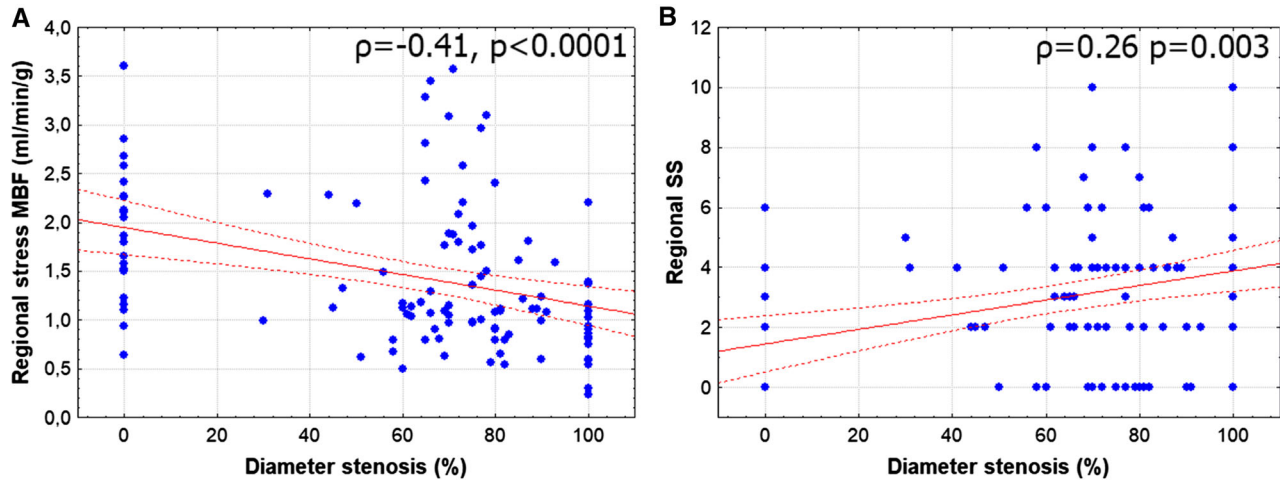


Figure 3. Correlation between regional AC stress MBF and perfusion abnormalities and coronary stenosis. Regional MBF (A) shows the best correlation in the detection of coronary stenosis, when compared to regional perfusion score (B) in the same territory.

MFR, as an index which correlates with stenosis severity and CAD extent.

More than this, the results of the present study indicate that stress MBF, as previously reported in PET studies, may be better used in the evaluation of patients with suspected CAD, increasing the sensitivity and specificity in detecting not only IVD, but also MVD.³⁵

As previously demonstrated with PET,²⁵ the mean values of stress MBF and MFR obtained in this study, were statistically lower in patients with MVD than in those with IVD or in patients without significant stenosis. This data is of relevance, because MBF and MFR threshold values obtained in this study can be used in addition to the presence of stress perfusion abnormalities to increase the accuracy in identifying patients with higher risk.

Furthermore, after adjusting for clinical parameters and other myocardial perfusion indexes only stress MBF remained an independent predictor of MVD, underlined the impact of this variable in the evaluation of CAD extent.

This result is particularly relevant if considering the consistent number of “difficult” patients with diabetes, obesity, known MVD where the use of functional tests is necessary for the evaluation of risk stratification and where the detection of abnormal MBF in more territories can be of help in the clinical decision making. On the other hand, the extrapolation of our result to populations with a lower prevalence of obstructive CAD (i.e. general population) should be careful because of global MBF and MFR values in the cases of both multivessel CAD and microvascular dysfunction may be reduced.

Our results suggest that the use of CZT MBF quantification could be useful to identify high-risk CAD patients. More multicenter and multivendor studies are needed to confirm these data before applying it routinely.

LIMITATION

The power of this study is limited by the consecutive nature of the enrollment and the small number of patients. The number of affected vessels was established on quantitative ICA data without the use of FFR. No comparison of CZT values with PET was done. In IVD group patients there were no stenosis in RCA that could be a bias in regional analysis. In this study we use stable CAD subjects without obstructive CAD and with risk factors as a control group. It could result in some underestimation of intergroup difference in terms of stress MBF and MFR values. Most of patients in this study have obstructive CAD that may affect the values of accuracy. The low range of stress flow values was obtained by CZT compared to previous PET studies. It could be related to different acquisition technique, intrinsic tracer limitation and flow model issues. It determines the necessity in certain cut-off values for identification of high-risk patients by using CZT SPECT.

NEW KNOWLEDGE GAINED

On global and regional level, quantitative myocardial perfusion parameters allowed to identify high-risk disease better than semiquantitative indexes. Higher

accuracy of stress MBF to detect high-risk patients compared to low risk patients has been shown.

CONCLUSIONS

The use of absolute myocardial blood flow analysis with the CZT camera may identify high risk patients with multivessel disease. This approach could be used in clinical practice, increasing the accuracy in the evaluation of patients with known or suspected coronary artery disease.

Disclosures

Authors did not have financial, personal or professional relationships with other people or organizations. Authors declare that they have no conflicts of interest.

References

1. Gimelli A, Liga R, Duce V, Kusch A, Clemente A, Marzullo P. Accuracy of myocardial perfusion imaging in detecting multivessel coronary artery disease: A cardiac CZT study. *J Nucl Cardiol* 2017;24:687-95. <https://doi.org/10.1007/s12350-015-0360-8>.
2. Schindler TH. Myocardial blood flow: Putting it into clinical perspective. *J Nucl Cardiol* 2016;23:1056-71. <https://doi.org/10.1007/s12350-015-0372-4>.
3. Driessen RS, Raijmakers PG, Stuijzand WJ, Knaapen P. Myocardial perfusion imaging with PET. *Int J Cardiovasc Imaging* 2017;33:1021-31. <https://doi.org/10.1007/s10554-017-1084-4>.
4. Imbert L, Poussier S, Franken PR, Songy B, Verger A, Morel O, et al. Compared performance of high-sensitivity cameras dedicated to myocardial perfusion SPECT: A comprehensive analysis of phantom and human images. *J Nucl Med* 2012;53:1897-903. <https://doi.org/10.2967/jnumed.112.107417>.
5. Ben Bouallègue F, Roubille F, Lattuca B, Cung TT, Macia J-C, Gervasoni R, et al. SPECT myocardial perfusion reserve in patients with multivessel coronary disease: Correlation with angiographic findings and invasive fractional flow reserve measurements. *J Nucl Med* 2015;56:1712-7. <https://doi.org/10.2967/jnumed.114.143164>.
6. Agostini D, Roule V, Nganoa C, Roth N, Baavour R, Parienti J-J, et al. First validation of myocardial flow reserve assessed by dynamic ^{99m}Tc-Sestamibi CZT-SPECT camera: Head to head comparison with ¹⁵O-water PET and fractional flow reserve in patients with suspected coronary artery disease. The WATERDAY study. *Eur J Nucl Med Mol Imaging* 2018;45:1079-90. <https://doi.org/10.1007/s00259-018-3958>.
7. Zavadvovsky KV, Mochula AV, Boshchenko AA, Vrublevsky AV, Baev AE, Krylov AL, et al. Absolute myocardial blood flows derived by dynamic CZT scan vs invasive fractional flow reserve: Correlation and accuracy. *J Nucl Cardiol* 2019. <https://doi.org/10.1007/s12350-019-01678-z>.
8. Nkoulou R, Fuchs TA, Pazhenkottil AP, Kuest SM, Ghadri JR, Stehli J, et al. Absolute myocardial blood flow and flow reserve assessed by gated SPECT with cadmium-zinc-telluride detectors using ^{99m}Tc-tetrofosmin: Head-to-head comparison with ¹³N-ammonia PET. *J Nucl Med* 2016;57:1887-92. <https://doi.org/10.2967/jnumed.115.165498>.
9. Miyagawa M, Nishiyama Y, Uetani T, Ogimoto A, Ikeda S, Ishimura H, et al. Estimation of myocardial flow reserve utilizing an ultrafast cardiac SPECT: Comparison with coronary angiography, fractional flow reserve, and the SYNTAX score. *Int J Cardiol* 2017;244:347-53. <https://doi.org/10.1016/j.ijcard.2017.06.012>.
10. Henzlva MJ, Duvall WL, Einstein AJ, Travin MI, Verberne HJ. ASNC imaging guidelines for SPECT nuclear cardiology procedures: Stress, protocols, and tracers. *J Nucl Cardiol* 2016;23:606-39. <https://doi.org/10.1007/s12350-015-0387-x>.
11. Farooq V, Van Klaveren D, Steyerberg EW, Meliga E, Vergouwe Y, Chieffo A, et al. Anatomical and clinical characteristics to guide decision making between coronary artery bypass surgery and percutaneous coronary intervention for individual patients: Development and validation of SYNTAX score II. *Lancet* 2013;381:639-50. [https://doi.org/10.1016/s0140-6736\(13\)60108-7](https://doi.org/10.1016/s0140-6736(13)60108-7).
12. Cerqueira MD, Weissman NJ, Dilsizian V, Jacobs AK, Kaul S, Laskey WK, et al. Standardized myocardial segmentation and nomenclature for tomographic imaging of the heart: A statement for healthcare professionals from the cardiac imaging. *Circulation* 2002;105:539-42. <https://doi.org/10.1161/hc0402.102975>.
13. Wells RG, Marvin B. Measuring SPECT myocardial blood flow at the University of Ottawa Heart Institute. *J Nucl Cardiol* 2020. <https://doi.org/10.1007/s12350-020-02102-7>.
14. Leppo JA, Meerdink DJ. Comparison of the myocardial uptake of a technetium-labeled isonitrite analogue and thallium. *Circ Res* 1989;65:632-9. <https://doi.org/10.1161/01.res.65.3.632>.
15. Yoshida K, Mullani N, Gould KL. Coronary flow and flow reserve by PET simplified for clinical applications using rubidium-82 or nitrogen-13-ammonia. *J Nucl Med* 1996;37:1701-12.
16. Camici PG, Rimoldi OE. The clinical value of myocardial blood flow measurement. *J Nucl Med*. 2009. <https://doi.org/10.2967/jnumed.108.054478>.
17. Ziadi MC. Myocardial flow reserve (MFR) with positron emission tomography (PET)/computed tomography (CT): Clinical impact in diagnosis and prognosis. *Cardiovasc Diagn Ther* 2017;7:206-18. <https://doi.org/10.21037/cdt.2017.04.10>.
18. Hsu B, Chen FC, Wu TC, Huang WS, Hou PN, Chen CC, et al. Quantitation of myocardial blood flow and myocardial flow reserve with ^{99m}Tc-Sestamibi dynamic SPECT/CT to enhance detection of coronary artery disease. *Eur J Nucl Med Mol Imaging* 2014;41:2294-306. <https://doi.org/10.1007/s00259-014-2881-9>.
19. Giubbini R, Bertoli M, Durmo R, Bonacina M, Peli A, Faggiano I, et al. Comparison between ¹³NH₃-PET and ^{99m}Tc-tetrofosmin-CZT SPECT in the evaluation of absolute myocardial blood flow and flow reserve. *J Nucl Cardiol* 2019. <https://doi.org/10.1007/s12350-019-01939-x>.
20. Wells RG, Timmins R, Klein R, Lockwood J, Marvin B, De Kemp RA, et al. Dynamic SPECT measurement of absolute myocardial blood flow in a porcine model. *J Nucl Med* 2014;55:1685-91. <https://doi.org/10.2967/jnumed.114.139782>.
21. Kaufmann PA, Camici PG. Myocardial blood flow measurement by PET: Technical aspects and clinical applications. *J Nucl Med* 2005;46:75-88.
22. Gould KL, Johnson NP, Bateman TM, Beanlands RS, Bengel FM, Bober R, et al. Anatomic versus physiologic assessment of coronary artery disease: Role of coronary flow reserve, fractional flow reserve, and positron emission tomography imaging in revascularization decision-making. *J Am Coll Cardiol* 2013. <https://doi.org/10.1016/j.jacc.2013.07.076>.
23. Camici PG, Crea F. Coronary microvascular dysfunction. *N Engl J Med* 2007;356:830-40. <https://doi.org/10.1056/nejmra061889>.

24. Gupta A, Taqueti VR, van de Hoef TP, Bajaj NS, Bravo PE, Murthy VL, et al. Integrated noninvasive physiological assessment of coronary circulatory function and impact on cardiovascular mortality in patients with stable coronary artery disease. *Circulation* 2017;136:2325-36. <https://doi.org/10.1161/circulationaha.117.029992>.
25. Bom MJ, van Diemen PA, Driessen RS, Everaars H, Schumacher SP, Wijmenga J-T, et al. Prognostic value of [¹⁵O]H₂O positron emission tomography-derived global and regional myocardial perfusion. *Eur Heart J Cardiovasc Imaging* 2019. <https://doi.org/10.1093/ehjci/jez258>.
26. Murthy VL, Naya M, Foster CR, Hainer J, Gaber M, Di Carli G, et al. Improved cardiac risk assessment with noninvasive measures of coronary flow reserve. *Circulation* 2011;124:2215-24. <https://doi.org/10.1161/circulationaha.111.050427>.
27. Joutsiniemi E, Saraste A, Pietilä M, Mäki M, Kajander S, Ukkonen H, et al. Absolute flow or myocardial flow reserve for the detection of significant coronary artery disease? *Eur Heart J Cardiovasc Imaging* 2014;15:659-65. <https://doi.org/10.1093/ehjci/jez274>.
28. Danad I, Uusitalo V, Kero T, Saraste A, Rajmakers PG, Lammertsma AA, et al. Quantitative assessment of myocardial perfusion in the detection of significant coronary artery disease: Cutoff values and diagnostic accuracy of quantitative [¹⁵O]H₂O PET imaging. *J Am Coll Cardiol* 2014;64:1464-75. <https://doi.org/10.1016/j.jacc.2014.05.069>.
29. Juárez-Orozco LE, Alexanderson E, Dierckx RA, Boersma HH, Hillege JL, Zeebregts CJ, et al. Stress myocardial blood flow correlates with ventricular function and synchrony better than myocardial perfusion reserve: A nitrogen-13 ammonia PET study. *J Nucl Cardiol* 2018;25:797-806. <https://doi.org/10.1007/s12350-016-0669-y>.
30. Fiechter M, Ghadri JR, Gebhard C, Fuchs TA, Pazhenkottil AP, Nkoulou RN, et al. Diagnostic value of ¹³N-ammonia myocardial perfusion PET: Added value of myocardial flow reserve. *J Nucl Med* 2012;53:1230-4. <https://doi.org/10.2967/jnumed.111.101840>.
31. Kajander SA, Joutsiniemi E, Saraste M, Pietilä M, Ukkonen H, Saraste A, et al. Clinical value of absolute quantification of myocardial perfusion with ¹⁵O-water in coronary artery disease. *Circ Cardiovasc Imaging* 2011;4:678-84. <https://doi.org/10.1161/ircimaging.110.960732>.
32. Berman DS, Kang X, Slomka PJ, Gerlach J, de Yang L, Hayes SW, et al. Underestimation of extent of ischemia by gated SPECT myocardial perfusion imaging in patients with left main coronary artery disease. *J Nucl Cardiol* 2007;14:521-8. <https://doi.org/10.1016/j.nuclcard.2007.05.008>.
33. Ben-Haim S, Murthy VL, Breault C, Allie R, Sitek A, Roth N, et al. Quantification of myocardial perfusion reserve using dynamic SPECT imaging in humans: A feasibility study. *J Nucl Med* 2013;54:873-9. <https://doi.org/10.2967/jnumed.112.109652>.
34. Hyafil F, Gimelli A, Slart RHJA, Georgoulas P, Rischpler C, Lubberink M, et al. EANM procedural guidelines for myocardial perfusion scintigraphy using cardiac-centered gamma cameras. *Eur J Hybrid Imaging* 2019;3:11. <https://doi.org/10.1186/s41824-019-0058-2>.
35. Schindler TH. Positron-emitting myocardial blood flow tracers and clinical potential. *Prog Cardiovasc Dis* 2015;57:588-606. <https://doi.org/10.1016/j.pcad.2015.01.001>.

Publisher's Note Springer Nature remains neutral with regard to jurisdictional claims in published maps and institutional affiliations.